Extension of spread-slump formulae for yield stress evaluation

Alexandre Pierre, Christophe Lanos, Patrice Estellé

EXTENSION OF SPREAD-SLUMP FORMULAE FOR YIELD STRESS EVALUATION

Alexandre Pierre [1,2], Christophe Lanos [1], Patrice Estellé [1,*]

[1] UEB, LGCGM EA3913, Equipe Matériaux et Thermo-Rhéologie, Université Rennes 1, 3 rue du Clos Courtel, BP 90422, 35704 Rennes Cedex 7, France

[2] UEB-LIMATB, ECOMATH, Université de Bretagne Sud, Centre de Recherche de St Maudé, 56321 Lorient, France

* Corresponding author

Email: patrice.estelle@univ-rennes1.fr
Tel: +33 (0) 2 23 23 42 00
Fax: +33 (0) 2 23 23 40 51

Abstract:

This paper provides a new model to evaluate the yield stress of suspensions, slurries or pastes, based on the release of a finite volume of material onto a horizontal surface. Considering the height (h) and the radius (R) of the sample at the flow stoppage, two asymptotic regimes, where h>R or h<R, lead to different analytical models that allow the determination of yield stress. Experimental observations show typical sample shape at stoppage between slump (h>R) and spread (h<R). Based on these observations, we have developed a new analytical model to evaluate accurately the yield stress of materials in this intermediate regime. The validity of this model was evaluated from data obtained using various Carbopol® dispersions. The yield stress measured with the proposed model was compared with the yield stress evaluated from shear flow curves obtained with roughened plate/plate geometry fitted to the Herschel-Bulkley model. Results show the relevance of the proposed model which that can be applied in the range between models used for the two asymptotic regimes.

Keywords: Yield stress, Slump test, Intermediate regime, Spread flow, Rheology

Résumé:

Cet article présente un nouveau modèle d'évaluation du seuil de mise en écoulement pour des fluides complexes tel que des suspensions, pâtes ou coulis. Nous proposons d'évaluer le seuil par un essai d'écoulement libre du matériau sur une surface plane. Actuellement,

deux principaux régimes d'écoulement amenant à deux solutions distinctes sont considérés en prenant en compte la hauteur h et le rayon R du matériau à l'arrêt (h>R ou h<R). Nous avons observé un régime intermédiaire d'écoulement, entre le régime d'affaissement (slump), caractérisée par h>R et le régime d'étalement (spread) où h<R. De ce fait, nous proposons un modèle analytique conduisant à une solution unique pour évaluer le seuil de mise en écoulement. Le modèle est validé en comparant les résultats obtenus sur différents gels de Carbopol®. Les seuils évalués par étalement sont comparés aux seuils de mise en écoulement évalués en adaptant le modèle d'Herschel-Bulkley sur les courbes d'écoulement obtenus avec un rhéomètre équipé d'une géométrie plan-plan rugueuse. Les résultats du modèle sont très pertinents, assurant une continuité de l'interprétation entre les deux régimes asymptotiques.

1 INTRODUCTION

Many industrial and natural suspensions behave as yield stress materials that flow only when they are subjected to a minimum shear stress. From cosmetics [1] to cement-based materials [2-4], the flow behaviour of such materials is governed by the magnitude of their yield stress. Therefore, measuring this yield stress is a major issue for many industries and applications [5]. It is possible to evaluate the shear stress in several ways [6-7]; amongst these is a simple and useful method that consists of the release of a finite volume of material onto a horizontal surface. The material sample is initially placed in a mould, which is then lifted, and the material flows under gravitational force. Due to the ratio between the radius R and the height h of the flowed volume, this test is referred to as 'slump' for h>R, and 'spread flow' for h<R respectively [8]. The advantage of this manual test is that it can be used on construction sites or in the development of mix-design.

This test was initially developed for civil engineering applications using a mould with a conical geometry [9]. This test is often associated with Abrams, but it is believed that, according to Bartos et al. [9] and Wallevik [11], Chapman [10] was the first to use it. Published literature in this field note that the ASTM Abrams cone [12] is applicable to quantify the rheology of fresh concrete as the size of the coarse aggregate used in concretes is large. Kandro [13] subsequently developed a new geometry, called the 'mini slump cone test', to study the influence of water-reducing admixtures on rheology of cement paste. Mini-cone has since been widely used for cement pastes, grouts or suspensions with low yield stress [14]. There is also a preference to use cylindrical moulds with such materials [15-16].

Studies relating to the evaluation of the yield stress from slump and spread measurements have been previously reported. Applying a mechanical approach Murata [17] established a relation between the height of the material at the end of the slump test and the yield stress of

the tested material. This relation, obtained with a conical geometry, was improved by Christensen [18], by the introduction of dimensionless quantities and correcting an integration error in the Murata model. In these works, it is considered that the material in the upper part of the cone does not flow. In the lower part, the stress induced by the self-weight of the material is higher than the yield stress and flowing occurs. Finally, it would appear that the height of the flowing material decreases until the stress is equal to the yield stress and consequently the flow stops.

The influence of the mould geometry used to perform the test has also been discussed. Rajani et al. [19] and Schowalter et al. [20] worked on the slump test using a conical geometry. They established a correlation between the sample height at the flow stoppage and the yield stress that does not depend on the initial geometry of the cone. Later, Chandler [21] adapted the slump test to a cylindrical mould without obtaining an analytical relationship between the slump and the material's yield stress

Pahias et al. [22] were the first to link the yield stress, evaluated from a vane rheometer, to the yield stress obtained from the slump test. They also reported that the slump does not depend on the mould lift velocity and the surface on which the slump is performed. Clayton et al. [16] compared conical and cylindrical geometries taking as a reference the yield stress obtained with a vane test using the Nguyen and Boger technique [23]. Clayton et al. [16] reported improved results using a cylindrical mould rather than a conical mould. In addition, they showed that the final shape of the material depends on the height of a conical geometry mould. They also reported that slump test results were not influenced by the height of the cylindrical mold for yield stress value lower than 250 Pa.

From numerical simulations, Davidson et al. [24] predicted that the material's height decreased more quickly with time as the yield stress of the fluid decreased. Clayton et al. [16], Pashias et al. [22], and Saak et al. [25] showed that the final results were independant of the initial shape of the mould, notably for large slumps corresponding to low yield stress values.

These previous theoretical developments were extended by Roussel and Coussot [8], who neglected viscous, inertia and surface tension effects. They proposed analytical solutions for the slump and spread flow regimes, and showed that these two regimes could be considered as elongational flow and pure shear flow respectively. These analytical solutions were favourably compared to numerical simulations [8] and experimental data on cement paste and concrete [14]. Comparison of yield stress values obtained from vane concrete rheometer and slump was also reported by Estellé and Lanos [2]. An attempt was also made to introduce surface tension effects in spread flow [14], the proposed solution was limited to one

cement paste. Roussel and Coussot [8] noted that the two analytical models did not provide the same yield stress values in the case of flow behaviour that occurred between elongational and shear flow. In addition, Flatt et al. [26] found a divergence between both models for yield stress value close to 100 Pa.

As reported above and to our knowledge, there are no reported works concerning the yield stress evaluation in a typical intermediate shape at the flow stoppage, i.e. between slump and spread. However as we observed in this study this transitional condition can occur with variation of yield stress. The aim of the present paper is to extend previously published formulae of limiting cases of slump and spread flow [8] and to correctly evaluate the yield stress of the material whatever the flow regime, volume of the sample or the shape of the mould.

The Carbopol® dispersions are used in this study to provide a simple yield stress model material. The experiments for rheological and slump/spread measurements are set out in section 2. Experimental results and observations are reported in section 3, where a schematic representation is proposed for the flow typology between spread and slump. The theoretical framework of the proposed model is developed in section 4 and finally validation of the model is presented and discussed in section 5.

2 MATERIALS AND MEASUREMENTS

2.1 Material and suspensions preparation

Carbopol® 676 was supplied by Lubrizol in a powder form. This material, according to the manufacturer's specification, is a highly crosslinked poly-acrylic acid polymer that is synthesized in benzene. A starting Carbopol® suspension with a weight fraction of 1-2 % was prepared, as proposed in [27], by slowly adding the powder to distilled water. The mixture was stirred slowly with a variable speed mixer to disperse the powder and reduce the presence of air bubbles within the suspension. The dispersion was then neutralized with NaOH. This starting suspension was then divided and distilled water was added to obtain samples with a range of yield stress between 5 and 100 Pa. The pH of the suspensions was 7±0.1, indicating that the yield stress of Carbopol® suspension only depends on the water content. The densities of the Carbopol® suspensions ranged 1012 to 1030 $kg.m^{-3}$, the density increased with increasing yield stress. These values were very close to the density of water due to the low polymer concentration being used. Each sample was stored in a container and conserved at room temperature before being tested.

2.2 Rheological measurements

Rheological measurements of Carbopol® dispersions were performed using a rheometer (Malvern Kinexus®) in a parallel plate configuration under a controlled temperature of 20° C. The temperature was controlled using a Peltier temperature control device located below the lower plate. All experiments were conducted with a 40 mm diameter plate and a constant gap of 1.5 mm. Sandpaper was glued to both plates to prevent slippage. Each test sample was transferred to the lower plate; the upper plate was adjusted to achieve the required sample gap. The excess of samples was then removed. The sample was presheared at 5 s^{-1} for 20 s, then was left to rest for 40 s. Thereafter, rate-controlled measurements were carried out by applying a logarithmic up-and-down shear rate ramp ranging from 10^{-2} to 1000 s^{-1} over 2 minutes. The tests were repeated at least once to both verify the repeatability of the rheological measurement and the suspension stability with time.

2.3 Spreading measurements

Spreading flow tests were performed using a cylinder mould 56.5 mm in height and 97 mm internal diameter. The cylindrical mould was placed on a plane glass plate that had been previously cleaned with acetone; the mould was then filled with the Carbopol® dispersion. The cylinder was lifted and the suspension flowed under gravity on the plate. The dimensions of the suspension sample after flow stoppage were carefully measured to the nearest 0.5 mm, with a rule. The final height and diameters of the sample used for the yield stress calculation were the mean value of two measurements made in two perpendicular directions. Based on the equations developed further, the uncertainty in sample dimensions measurement leads to a maximum relative deviation for yield stress evaluation less than 3%. The spreading flow measurement was repeated twice at 20 ± 1 ℃.

3 EXPERIMENTAL RESULTS

3.1 Shear flow behavior

Figure 1 shows the shear flow behaviour of the Carbopol® dispersion with a yield stress of 62 Pa. The Carbopol® dispersion is not thixotropic as the increasing and decreasing curves are superimposed within the shear rate range investigated. A transition from an elastic solid behaviour to a liquid behaviour was also observed under the increasing shear rate and for shear rate lower than 0.1 s^{-1} (figure 1). Similar trends were observed for other suspensions regardless of the yield stress. As expected and is widely reported in literature [28-29], the Carbopol® suspensions behave as a simple yield stress fluid with shear-thinning behaviour, which can be well modelled using a Herschel-Bulkley model [30]:

$$\tau = \tau_c + \eta\,\dot{\gamma}^n \quad (1)$$

Where τ is the shear stress, τ_c is the yield stress, η is the consistency and n is the flow index behaviour.

3.2 Spreading behaviour

Figure 2 illustrates the spreading flows tests that were performed using four different Carbopol® suspensions. The shape at flow stoppage was strongly dependent on the yield stress. For a weak yield stress, the sample radius is much higher than the sample height, this shape being representative of spreading flow [8]. Increasing the yield stress, the height/radius ratio decreases, leading to intermediate flow regime. Finally for a yield stress of 100 Pa, the flow tends to the slump regime. The images shown in figure 2 show the upper central part of the sample, subsequently referred to as the 'hat', preserves a cylindrical form even if its height varies with the yield stress of the dispersion. This configuration, between slump and spread, depends on the yield stress of the Carbopol® suspensions.

Based on this experimental observation, a schematic shape of the sample at the flow stoppage is proposed in figure 3. The schematic representation consists of a central part where the maximum height of the sample is reached. This central part is characterized by the the dimensions R_0 and $h = h_0 + h(R_0)$. The radius and the height of the 'hat' are respectively denoted R_0 and h_0. It is considered that a radius R and a maximum height $h(R_0)$ characterize the peripheral part around the central part.

Figure 4 summarises the results of the preceding tests, the figure shows the measured height in the centre of the samples at flow stoppage, with respect to both the radii of the central part R_0 and the peripheral part R. This procedure was carried out for all the prepared Carbopol® suspensions. As expected, figure 4 shows that the radius of the peripheral part increases with decreasing yield stress. Figure 4 also shows the variation of the radius of the hat (R_0) is limited to 1 cm even for high spread values. It can therefore be considered that the central zone, the 'hat', has a reasonably constant radius which is close to that of the mould, and that its height decreases with decreasing yield stress of the suspension. These observations led to the sample schematic shape represented in figure 3 that was used for the model development set out in section 5.

4 THEORY

4.1 Generalities

The mechanical laws of an incompressible material with a yield stress flowing on a plane surface are described in the following section. The flow is described in cylindrical coordinates

attached to the horizontal solid surface (r, θ, z). The cylindrical geometry used for the spreading flow is shown in figure 5. The axisymmetry of the problem implies that there is no tangential motion in a specific direction (V_θ) and that the variables do not depend on θ. It is also assumed that the material flow stoppage occurs when the shear stress in the material is equal to or lower than the yield stress. As reported in the introduction, the viscosity of the material, inertia and surface tension effects at stoppage, are also neglected [8].

The strain rate tensor is:

$$\mathbf{D} = \begin{bmatrix} \frac{\partial V_r}{\partial r} & 0 & \frac{1}{2}\left(\frac{\partial V_z}{\partial r} + \frac{\partial V_r}{\partial z}\right) \\ 0 & \frac{V_r}{r} & 0 \\ \frac{1}{2}\left(\frac{\partial V_z}{\partial r} + \frac{\partial V_r}{\partial z}\right) & 0 & \frac{\partial V_z}{\partial z} \end{bmatrix} \quad (2)$$

Equation (2) is associated to a three dimensional criterion, known as the von Mises yielding criterion. This criterion is commonly used for solids and can also be used to predict jamming of yield stress materials and Carbopol® dispersions [31]:

$$\mathbf{D} = 0 \Leftrightarrow \sqrt{-T_{II}} < \tau_c \quad (3)$$

where T_{II} is the second invariant of the extra stress tensor and τ_c is the yield stress.

It is assumed that the constitutive equation beyond yielding can be expressed in the general form [32]:

$$\mathbf{T} = -p\mathbf{I} + \mathbf{T}' = -p\mathbf{I} + \frac{\tau_c}{\sqrt{-D_{II}}}\mathbf{D} \quad (4)$$

Where $\mathbf{T}$ is the stress tensor, which can vary with the flow regime, p is the pressure, and $\mathbf{T}'$ is the extra stress tensor. $D_{II} = 1/2\,((\mathrm{tr}\,D)^2 - \mathrm{tr}\,(D^2))$ is the second invariant of the strain rate tensor and $\mathbf{I}$ is the identity tensor.

4.2 Slump flow

The stress variations in the radial variation are negligible compared with those in the vertical direction [8], this follows from the assumption that the flow is mainly elongational and thus, in the vertical direction, the stress results from the weight of the material above and is equal to $-\rho g(h_0 + h(R_0) - z)$ at a height z.

The pressure p, at $z = 0$, is defined as follows:

$$p = -\frac{tr\,\mathbf{T}}{3} = -\frac{\rho g(h_0 + h(R_0))}{3} \tag{5}$$

Where ρ is the material's density and g is acceleration due to gravity and the extra stress tensor is:

$$\mathbf{T}' = \mathbf{T} - \frac{1}{3}\mathrm{tr}(\mathbf{T})\mathbf{I} \tag{6}$$

Equations (5) and (6) yield:

$$\mathbf{T}' = \begin{bmatrix} \frac{1}{3}\rho g(h_0 + h(R_0)) & 0 & 0 \\ 0 & \frac{1}{3}\rho g(h_0 + h(R_0)) & 0 \\ 0 & 0 & -\frac{2}{3}\rho g(h_0 + h(R_0)) \end{bmatrix} \tag{7}$$

In tangential and radial directions, the stress is equal to zero. By considering equation (4), the stress tensor is expressed as:

$$\mathbf{T} = -\frac{\rho g(h_0 + h(R_0))}{3}\mathbf{I} + \frac{\rho g(h_0 + h(R_0))}{3}\begin{bmatrix} 1 & 0 & 0 \\ 0 & 1 & 0 \\ 0 & 0 & -2 \end{bmatrix} \tag{8}$$

The second invariant of the extra-stress tensor T_{II} is calculated as:

$$T_{II} = -\frac{1}{3}(\rho g(h_0 + h(R_0)))^2 \tag{9}$$

Consequently, for small deformation, and considering that flow stoppage results in the height $h_0 + h(R_0)$ at which the von Mises criterion is exactly reached, the yield stress is finally obtained from equation (10) [8]:

$$\tau_c = \frac{\rho g(h_0 + h(R_0))}{\sqrt{3}} \tag{10}$$

4.3 Spreading flow

In the spread regime, the flowing sample is mainly submitted to a pure shear flow [8]. As the height of the sample is smaller compared to its radius (h<R), it is to be expected that the radial velocity is much larger to the vertical velocity ($v_z << v_r$). Thus, based on the lubrication approximation, the strain tensor reduces to equation (11) [8]:

$$\mathbf{D} = \begin{bmatrix} 0 & 0 & \frac{1}{2}\left(\frac{\partial \mathrm{V_r}}{\partial \mathrm{z}}\right) \\ 0 & 0 & 0 \\ \frac{1}{2}\left(\frac{\partial \mathrm{V_r}}{\partial \mathrm{z}}\right) & 0 & 0 \end{bmatrix} \tag{11}$$

If the material is in spread regime and neglecting inertia effect, only the tangential stress component τ_{rz} is significant at $z = 0$ in the extra stress tensor. Considering equations (4) and (11), the momentum equations reduce to:

$$0 = -\frac{\partial p}{\partial r} + \frac{\partial \tau_{rz}}{\partial z} \; ; 0 = -\rho g - \frac{\partial p}{\partial z} \tag{12}$$

Considering that at material stoppage the stress tensor component is equal to τ_c ($\tau_{rz}(0) \rightarrow \tau_c$), the yield stress can be derived from the momentum equation and expressed as follows:

$$\tau_c = \rho g h \frac{dh}{dr} \tag{13}$$

With the boundary conditions ($h(R) = 0$), the sample height as a function of the distance r from the sample centre can be obtained from the previous equation:

$$h(r) = \left(\frac{2\tau_c (R - r)}{\rho g}\right)^{1/2} \tag{14}$$

The volume of the sample V_0 is:

$$V_0 = \int_0^R 2\pi r h(r) dr \tag{15}$$

Combining equations (14) and (15) leads to equation (16):

$$V_0 = 2\pi \sqrt{\frac{2\tau_c}{\rho g}} \frac{4}{15} R^{5/2} \tag{16}$$

Finally for the spread regime, the yield stress is expressed by equation (17) which was initially obtained by Roussel and Coussot [8] :

$$\tau_c = \frac{225\, \rho g}{128\, \pi^2\, R^5} {V_0}^2 \tag{17}$$

4.5 Intermediate regime: model development

Based on our experimental observations (figure 2), the volume of the mould V_0 can be expressed in terms of the volume of the central zone and the volume of the sample spreading around this central zone. This is expressed by equation (18):

$$V_0 = V_{spread} + \pi {R_0}^2 (h_0 + h(R_0)) \tag{18}$$

However, a question arises: what is the flow regime in the central zone?

Firstly it could be considered that the central zone is subjected to an elongational flow condition. Consequently the height of the central part is related to the yield stress of the material according to the equation (19):

$$h = (h_0 + h(R_0)) = \tau_c \frac{\sqrt{3}}{\rho g} \tag{19}$$

It could also be considered that the central zone can be decomposed into two parts as shown in figure 3. The upper part, previously named the 'hat', is assumed to reach the elongational flow condition at the base surface of the hat. Thus, according to [5]:

$$h_0 = \frac{\sqrt{3}\,\tau_c}{\rho g} \tag{20}$$

In the lower part, at stoppage, the stress state results from elongational flow and a pressure equilibrium induced by the peripheral zone and the weight of the hat. Consequently, in the peripheral zone, considering the boundary condition $h(R) = 0$ and replacing r by R_0 in equation (14), the balance equation at $r = R_0$ becomes:

$$h(R_0) = \sqrt{\frac{2\tau_c}{\rho g}}\ (R - R_0)^{1/2} \tag{21}$$

Combining equations (20) and (21), the height of the central part can finally be expressed as:

$$h = \frac{\sqrt{3}\,\tau_c}{\rho g} + \sqrt{\frac{2\tau_c}{\rho g}}\ (R - R_0)^{1/2} \tag{22}$$

Figure 6 shows a comparison of sample height at flow stoppage calculated with equations (19) and (22) with the measured sample height. It is worth noting that the yield stress values considered in equations (19) and (22) are obtained from fits of the Herschel-Bulkley model (equation (1)) to the shear flow data under decreasing ramp in shear rate. Figure 6 shows a reasonable agreement is obtained between the measurements and equation (22). This implies that the hat in the central zone is almost unsheared.

The volume of the sample spreading around the central zone is also expressed as:

$$V_{spread} = \int_{R_0}^{R} 2\pi r h(r) dr \tag{23}$$

Combining equations (14) and (23), and integrating leads to equation (24):

$$V_{spread} = \int_{R_0}^{R} 2\pi r h(r) dr\, 2\pi = \sqrt{\frac{2\tau_c}{\rho g}} \frac{4}{15} (R - R_0)^{5/2} + 2\pi \sqrt{\frac{2\tau_c}{\rho g}} \frac{2}{3} R_0 (R - R_0)^{3/2} \tag{24}$$

Based on the previous considerations, combining equations (18), (22) and (24) leads to equation (25):

$$0 = \left[\frac{8\pi}{15}(R - R_0)^{\frac{5}{2}} + \frac{4\pi}{3} R_0 (R - R_0)^{\frac{3}{2}} + \pi {R_0}^2 (R - R_0)^{\frac{1}{2}}\right] \sqrt{\frac{2\tau_c}{\rho g}} + \pi {R_0}^2 \sqrt{3} \frac{\tau_c}{\rho g} - V_0 \tag{25}$$

Equation (25) reduces to a second degree polynomial equation providing only one physical acceptable solution (i.e positive solution) given by equation (26):

$$\tau_c = \left(\frac{-b - \sqrt{b^2 - 4ac}}{2a}\right)^2 \tag{26}$$

With :

$$a = \frac{\pi {R_0}^2 \sqrt{3}}{\rho g} \tag{27}$$

$$b = \left[\frac{8\pi}{15}(R - R_0)^{\frac{5}{2}} + \frac{4\pi}{3} R_0 (R - R_0)^{\frac{3}{2}} + \pi {R_0}^2 (R - R_0)^{\frac{1}{2}}\right] \sqrt{\frac{2}{\rho g}} \tag{28}$$

$$\mathrm{c} = -\mathrm{V}_0 \tag{29}$$

5. Model validation

As shown in figure 7 and mentioned above, the yield stress values of the suspensions vary between 5 and 100 Pa depending on the water content of the Carbopol® suspension. These values are compared with the yield stress values obtained from the spreading measurement and calculated with equation (26), as set out in figure 7. For comparison purpose, the solution of the asymptotic spread regime (equation (17)) and slump regime (equation (10)) are also reported in figure 7.

In the yield stress range of 18 to 100 Pa, we observe a lower prediction of the yield stress with our model, which provided a better correlation with the values of yield stress evaluated

from the shear flow data. Therefore, in the regime between slump and spread, the proposed model, which takes into account the original shape at the end of the flow, ensures a precise prediction of the yield stress. Below yield stress values of 18 Pa, the material is mainly in spread regime and the hat's height is low. Consequently, Roussel's model [8] (equation (17)) is well adapted to predicting yield stress. For yield stress value close to 100 Pa, it is noted that our model yields a value close to the solution of equation (10) which corresponds to the elongational regime [8]. Above 100 Pa, the release of the suspensions tends towards a slump flow. It is worth noting that a change of mould geometry can affect the limits of the yield stress range linked to intermediate flow currently obtained.

5 CONCLUSION

It has been noted that a yield stress material flowing on a horizontal plane surface is not necessarily characteristic of a spread regime (R>h) or a slump regime (R<h) and can lead to an intermediate flow range between these two asymptotic regimes. Consequently, a new analytical model was developed to allow the determination of yield stress in this intermediate regime. The validity of the proposed model was assessed using Carbopol® dispersions. For the mould geometry used and in the yield stress range 20 to 100 Pa, the developed model for an intermediate flow leads to a reliable prediction of yield stress when compared to shear flow data.

References

[1] Brummer R: Rheology Essentials of Cosmetic and Food Emulsions, Springer, Berlin, (2005).

[2] Estellé P, Lanos C: High torque vane rheometer for concrete: principle and validation from rheological measurements, Appl. Rheol. 22 (2012) 12881.

[3] Nguyen TLH, Roussel N, Coussot P: Correlation between L-box test and rheological parameters of a homogeneous yield stress fluid, Cem. Conc. Res.36 (2006)1789‑1796.

[4] Perrot A, Lecompte T, Khelifi H, Brumaud C, Hot J, Roussel N: Yield stress and bleeding of fresh cement pastes, Cem. Conc. Res. 42 (2012) 937‑944.

[5] Coussot P: Rheometry of pastes, suspensions, and granular materials, Wiley, (2005).

[6] Nguyen QD, Akroyd TJ, De Kee DC, Zhu LX: Yield stress measurements in suspensions: an inter-laboratory study, Korea-Australia Rheol. J. 18 (1) (2006) 15‑24.

[7] Perrot A, Mélinge Y, Estellé P, Rangeard D, Lanos C: The back extrusion test as a technique for determining the rheological and tribological behaviour of yield stress fluids at low shear rates, Appl. Rheol. 21:5 (2011) 53642.

[8] Roussel N, Coussot P: “Fifty cent rheometer” for yield stress measurements: From slump to spreading flow, J. Rheol. 49:3 (2005) 705‑718.

[9] Bartos PJM, Sonebi M, Tamimi AK: Workability and Rheology of Fresh Concrete: Compendium of Tests, Report of RILEM TC 145-WSM (2002).

[10] Chapman CM: Method and Apparatus for Determining Consistency, ASTM V13 Part II Philadelphia (1913) 1045-1052.

[11] Wallevik JE: Relationship between the Bingham parameters and slump, Cem. Conc. Res. 36 (2006) 1214‑1221.

[12] ASTM Designation C143-90: Standard Test Method for Slump of Hydraulic Cement Concrete, Annual book of ASTM Standards (1896) 85‑87.

[13] Kandro DL: Influence of Water-Reducing Admixtures on Properties of Cement Paste-A Miniature Slump Test, Cem. Conc. Agg. 2:2 (1980) 85‑102.

[14] Roussel N, Stefani C, Leroy R: From mini-cone test to Abrams cone test: measurement of cement based materials yield stress using slump tests, Cem. Conc. Res. 35 (2005) 817‑822.

[15] Bouvet A, Ghorbel E, Bennacer R: The mini-conical slump flow test: Analysis and numerical study, Cem. Conc. Res. 40 (2010) 1517‑1523.

[16] Clayton S, Grice TG, Boger DV: Analysis of the slump test for on-site yield stress measurement of mineral suspensions, Int. J. Miner. Process. 70 (2003) 3‑21.

[17] Murata J: Flow and deformation of fresh concrete, Mat. Struct. 98 (1984) 117‑129.

[18] Christensen G: Modelling the flow of fresh concrete: the slump test, PhD Thesis (1991), Princeton University.

[19] Rajani. B, Morgenstern. N: On the yield stress of geotechnical materials from the slump test, Canadian Geotech. J. 28 (1991) 457-462.

[20] Schowalter W.R, Christensen G: Toward a rationalization of the slump test for fresh concrete: comparisons of calculations and experiments, J. Rheol. 42:4 (1998) 865-870.

[21] Chandler J.L: The stacking and solar drying process for disposal of bauxite tailings in Jamaica, Proceedings of the International Conference on Bauxite Tailings (1986), p. 101-105.

[22] Pashias N, Boger DV, Summers J, Glenister DJ: A fifty cent rheometer for yield stress measurement, J.Rheol 40:6 (1996) 1176-1189.

[23] Nguyen QD, Boger DV: Direct yield stress measurement with the vane method, J. Rheol 29 (1985) 335-347.

[24] Davidson MR, Khan NH, Yeow YL: Collapse of a cylinder of Bingham fluid, Proceedings of the 1999 International Conference on Computational Techniques and Applications, ANZIAM J. 42 (2000) 499-517.

[25] Saak AW, Jennings HM, Shah SP: A generalized approach for the determination of yield stress by slump and slump flow, Cem.Conc. Res. 34 (2004) 363-371

[26] Flatt RJ, Larosa D, Roussel N: Linking yield stress measurements: Spread test versus Viskomat, Cem. Conc. Res. 36 (2006) 99-109.

[27] Estellé P, Lanos C, Perrot A, Amziane S: Processing the vane shear flow data from Couette analogy, Appl.Rheol. 18:3 (2008) 34037.

[28] Piau JM: Carbopol gels: Elastoplastic and slippery glasses made of individual swollen sponges Meso-and macroscopic properties, constitutive equations and scaling laws, J.Non-Newt. Fluid Mech. 144 (2009) 1-29.

[29] Coussot P, Tocquer L, Lanos C, Ovarlez G: Macroscopic vs. local rheology of yield stress fluid, J.Non-Newt. Fluid Mech. 158 (2009) 85-90.

[30] Herschel WH, Bulkley R: Measurement of consistency as applied to rubber-benzene solutions, Am. Soc. Test Proc. 26 (1926) 621-633.

[31] Ovarlez G, Barral Q, Coussot P: Three-dimensional jamming and flows of soft glassy materials, Nat. Mat. 9 (2010) 115-119.

[32] Irgens F: Continuum Mechanics, Springer, (2008).

Figure Captions

Figure 1. Shear flow curve of the Carbopol® dispersion with a yield stress of 62Pa - ■: ramp up; □: ramp down.

Figure 2. Pictures of Carbopol® suspensions at the flow stoppage. Values of suspension yield stress: a) 21 Pa; b) 28 Pa; c) 62 Pa; d) 100 Pa.

Figure 3. Schematic representation of the suspension at flow stoppage under intermediate regime between spread and slump.

Figure 4. Heights measured at the stoppage of the material in the center part vs. the measured radii of the central part (□) and the measured radii of the peripheral part (Δ) measured. Carbopol® dispersions.

Figure 5. Initial cylinder shape and cylindrical coordinates.

Figure 6. Height calculated considering all the center part flowing as elongational (equation (19)) (●) and by distinguish the hat flow regime (○) (equation (21)) vs. height measured at the stoppage of the material at the central area. Carbopol® dispersions.

Figure 7. Present model for the intermediate regime (equation (26)) (□) ; Roussel's model considering spread flow (equation (17)) (■) and slump flow (equation (10)) (▲) vs the yield stress calculated with the Herschel-Bulkley model from shear stress-shear rates responses of the Carbopol® dispersions.

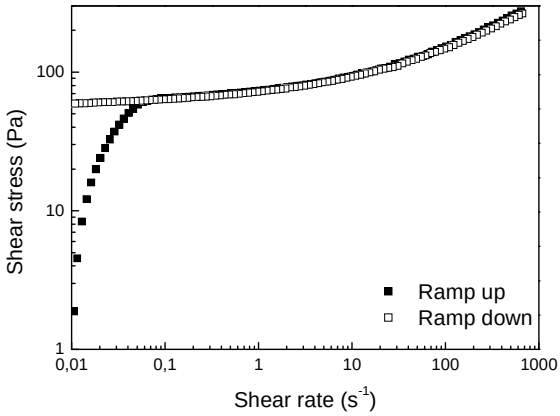

Figure 1. Shear flow curve of the Carbopol® dispersion with a yield stress of 62Pa ; ■: ramp up; □: ramp down.

a)

b)

c)

d)

Figure 2. Images of Carbopol® dispersions at the flow stoppage. Values of suspension yield stress: a) 21 Pa; b) 28 Pa; c) 62 Pa; d) 100 Pa.

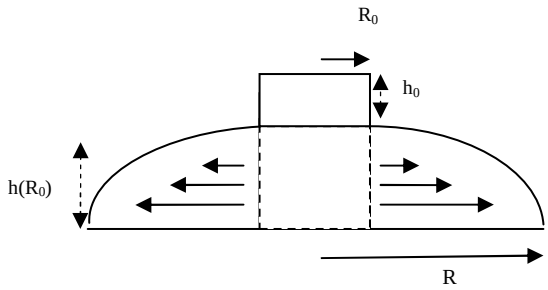

Figure 3. Schematic representation of the suspension at flow stoppage under intermediate regime between spread and slump.

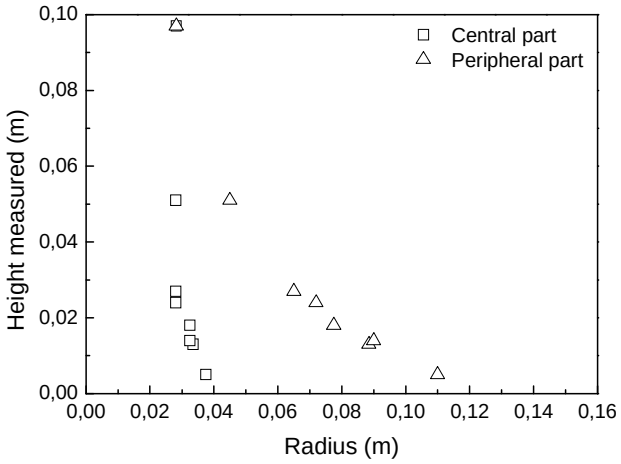

Figure 4. Heights measured at the stoppage of the material in the center part vs. the measured radii of the central part (□) and the measured radii of the peripheral part (Δ) measured. Carbopol® dispersions.

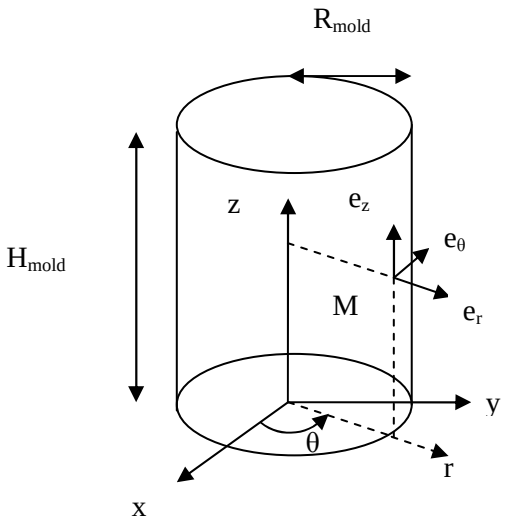

Figure 5. Initial cylinder shape and cylindrical coordinates.

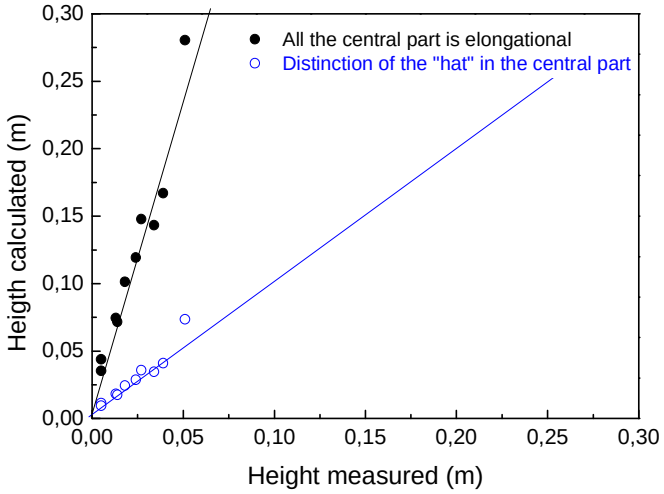

Figure 6. Height calculated considering all the center part flowing as elongational (equation (19)) (●) and by distinguishing the hat flow regime (○) (equation (21)) vs. height measured at the stoppage of the material at the central area. Carbopol® dispersions.

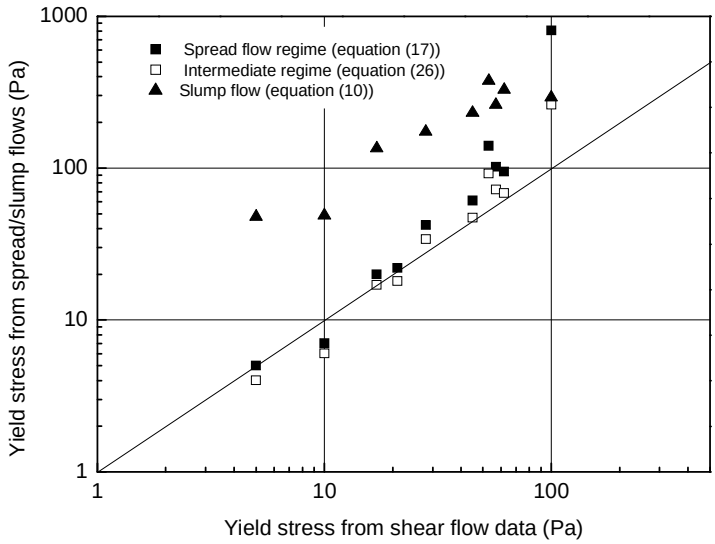

Figure 7. Present model for the intermediate regime (equation (26)) (□) ; Roussel's model considering spread flow (equation (17)) (■) and slump flow (equation (10)) (▲) vs the yield stress calculated with the Herschel-Bulkley model from shear stress-shear rates responses of the Carbopol® dispersions.